Tearout Strength of Concentrically Loaded Bolted Connections

NICOLO FRANCESCHETTI and MARK D. DENAVIT

ABSTRACT

The limit state of tearout can complicate the design of steel bolted connections since, in contrast to the limit states of bearing and bolt shear rupture, tearout strength can vary from bolt to bolt within a connection. Under the current AISC *Specification*, tearout strength is proportional to the clear distance, in the direction of force, between the edge of the hole and the edge of the adjacent hole or edge of the material. However, recent studies on concentrically loaded bolt groups have suggested that the use of clear distance may not accurately represent tearout strength and have proposed alternative lengths for use in strength equations. A reevaluation of the limit state of tearout in concentrically loaded bolt groups is presented in this work, including a thorough evaluation of the proposed alternative tearout lengths using a large database of previously published experimental work and new experiments with various edge distances and hole types. Equations with the alternative tearout lengths were found to be more accurate than those with clear distance, especially for small edge distances. Design recommendations including the alternative tearout lengths were developed. The results of this work increase understanding of the limit state of tearout and offer improved methods of evaluating this limit state in design.

Keywords: bolted connections, tearout, bearing, experiment, design.

INTRODUCTION

The current AISC *Specification for Structural Steel Buildings* (AISC, 2016), hereafter referred to as the AISC *Specification*, includes a user note, added in the 2010 edition (AISC, 2010), stating that the strength of a bearing-type bolt group in shear should be taken as the sum of the effective strengths of the individual bolts. The effective strength of a bolt is equal to the minimum strength computed for the limit states of bolt shear rupture, bearing, and tearout. By this method, it is possible, for example, to have the strength of a bolt group controlled by a combination of tearout for the bolts near an edge and bolt shear rupture for the remaining bolts. The possibility of this interaction of limit states is in contrast to a common practice where bolt shear rupture is treated as independent from bearing and tearout (Salmon et al., 2009). Evaluating the potential interaction of bolt shear rupture, bearing, and tearout complicates the design of bolt groups, primarily because the strength of an individual bolt for the limit state of tearout can vary from bolt to bolt within a group. Given the increased complexity and recently proposed alternative strength equations (Clements and Teh, 2013; Kamtekar, 2012), a reevaluation of the limit state of tearout is warranted to determine if changes can be made that lead to more accurate and efficient connection designs.

For bolts sufficiently far from edges of material and adjacent bolts, the strength of the connected material near the bolt is controlled by bearing. The limit state of bearing is characterized by plastic deformations of the connected material near the bolt hole and a long yield plateau in the load-deformation relationship. However, the connected material eventually ruptures with continued loading. In experimental testing, the peak load has been noted to occur upon reaching yield, prior to rupture or somewhere in between. However, once the yield plateau is reached, the variation in load is small.

Bearing strength has been observed to depend on the diameter of the bolt, the thickness of the connected material, and the tensile strength of the connected material. The edge distance (i.e., the distance from the center of hole to edge of connected material), when large, does not impact bearing strength. Near edges of material or adjacent bolts, the strength of the connected material near the bolt is less than the full bearing strength because one of several other limit states will control.

The primary limit state for connected material with smaller edge distance is tearout. Tearout is characterized by the rupture of the connected material on either side of the bolt. A similar failure mode is splitting, which involves a tensile rupture initiating at the end of the connected material. Some experiments have also shown modes of failure for bolted connections that include out-of-plane curling of unconfined plates. These three limit states are depicted in Figure 1.

Nicolo Franceschetti, Engineer, Palmer Engineering, Nashville, Tenn. (formerly Graduate Research Assistant, The University of Tennessee, Knoxville, Knoxville, Tenn.) Email: nfranceschetti@palmernet.com

Mark D. Denavit, Assistant Professor, The University of Tennessee, Knoxville, Knoxville, Tenn. Email: mdenavit@utk.edu (corresponding)

Paper No. 2020-07

AISC *Specification* Section J3.10 (2016) governs bearing and tearout strength at bolt holes. The nominal bearing strength of a bolt in a standard, oversize, or short-slotted hole, R_n, is given by Equations 1 and 2 (2016 AISC *Specification* Equations J3-6a and J3-6b).

$$R_n = 2.4dtF_u \tag{1}$$

$$R_n = 3.0dtF_u \tag{2}$$

where F_u is the specified minimum tensile strength of the connected material, d is the nominal bolt diameter, and t is the thickness of the connected material.

Equation 1 is used when deformation at the bolt hole at service load is a design consideration, whereas Equation 2 is used when deformation at the bolt hole at service load is not a design consideration. Significant bolt hole ovalization is expected to occur prior to reaching the full bearing strength of the connected material, which may limit the effectiveness of the connection. Frank and Yura (1981) identified ¼-in. deformation as a practical limit to define a bearing strength, which also prevents excessive ovalization.

The tearout strength of a bolt in a standard, oversize, or short-slotted hole is given by Equations 3 and 4 (2016 AISC *Specification* Equations J3-6c and J3-6d), where the distinction between Equations 3 and 4 is the same as that between Equations 1 and 2.

$$R_n = 1.2l_ctF_u \tag{3}$$

$$R_n = 1.5l_ctF_u \tag{4}$$

where l_c is the clear distance, in the direction of force, between the edge of the hole and the edge of the adjacent hole or edge of the material.

Provisions in the AISC *Specification* related to the limit state of tearout have changed over the various editions. In early editions—for example, the 1936 AISC *Specification* (AISC, 1936)—tearout was prevented by a limitation on edge distance. However, the limitation did not apply if there were three or more bolts in a line. In more recent editions—for example, the 1993 AISC *Specification* (AISC, 1993)—tearout was considered as a reduction to the bearing strength based on edge distance. An exception was also in place for these provisions. The reduction did not apply when there were two or more bolts in a line, a minimum edge distance of $1.5d$ was provided, a minimum spacing of $3d$ was provided, and deformation at the bolt hole was a design consideration. These exceptions were justified on the premise of load redistribution to the interior bolts or that sufficient interior bolts in a connection would diminish the effects of reduced strength at the edge bolts.

The form of the current provisions was introduced to the AISC *Specification* in the 1999 edition (AISC, 1999). An important change in these provisions was the use of the clear distance, l_c, for determining tearout strength instead of the edge distance. Also, no exceptions to the tearout check were provided.

This paper presents an investigation of tearout strength in concentrically loaded bolted connections. Recently proposed alternative strength equations (Clements and Teh, 2013; Kamtekar, 2012) are examined through comparisons to results from previously published experimental work and new experiments conducted by the authors. The comparisons provide a thorough evaluation of both the current and alternative strength equations. Based on the results, improvements to current design equations are recommended.

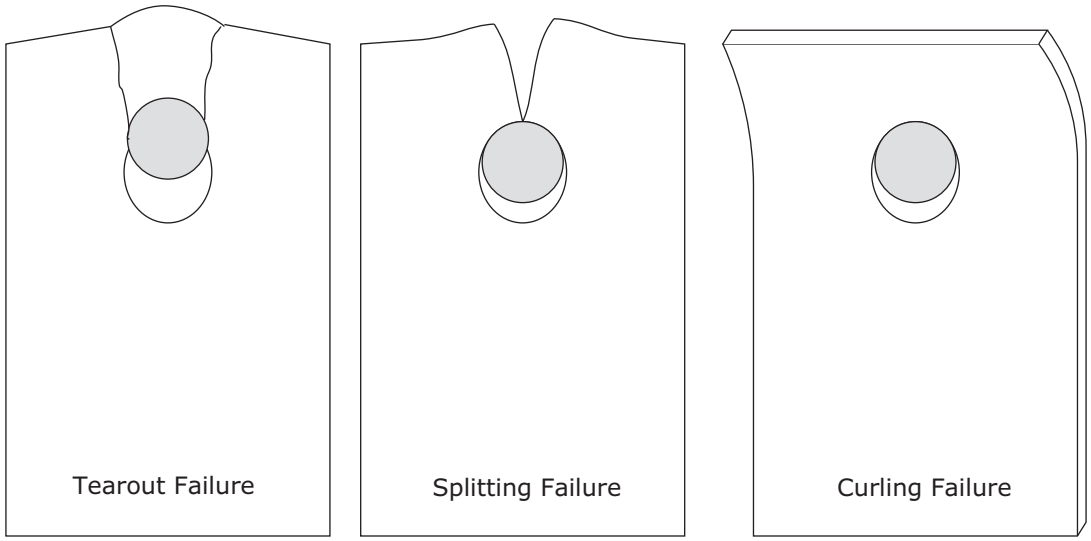

Fig. 1. Common failure modes of concentrically loaded bolted connections.

ALTERNATIVE TEAROUT LENGTHS

Under the current AISC *Specification* (AISC, 2016), strength for the limit state of tearout is based on the clear distance, in the direction of force, between the edge of the bolt hole and the edge of the adjacent hole or edge of the material. This distance is denoted as l_c. For the case illustrated in Figure 2, the clear distance is computed as a function of the edge distance, L_e, and the diameter of the hole, d_h:

$$l_c = L_e - \frac{d_h}{2} \tag{5}$$

Examination of experimental results has shown that the length of failure planes from specimens that exhibited tearout are somewhat longer than the clear distance. Researchers have proposed various alternative lengths that, when used in lieu of l_c, provide a more accurate assessment of strength. The first alternative tearout length that is investigated in this work, denoted as l_{v1}, was proposed by Kamtekar (2012) and is equal to the clear distance, in the direction of force, between the edge of the bolt hole and the edge of the adjacent hole or edge of the material along lines tangent to the bolt. For the case illustrated in Figure 2, l_{v1} is computed as:

$$l_{v1} = L_e - \frac{\sqrt{{d_h}^2 - d^2}}{2} \tag{6}$$

The second alternative tearout length that is investigated in this work, denoted as l_{v2}, was proposed by Clements and Teh (2013) and is equal to the average of the clear distance, l_c, and the edge distance, L_e. For the case illustrated in Figure 2, l_{v2} is computed as:

$$l_{v2} = L_e - \frac{d_h}{4} \tag{7}$$

Elliot et al. (2019) evaluated the use of l_{v1} and l_{v2} in strength equations for a small set of experiments that failed in tearout. They found them both to provide similarly improved predictions of tearout strength in comparison to current equations. They also evaluated alternative net areas for block shear rupture that are similar in concept to the alternative tearout lengths.

Other tearout lengths have been proposed (e.g., Duerr, 2006). However, differences among the lengths are slight. Also, some are more complicated than l_{v1} and l_{v2} to compute for general bolted connections. Therefore, this work focuses on evaluating l_c, l_{v1}, and l_{v2}.

EVALUATION OF PUBLISHED EXPERIMENTS

Hundreds of physical experimental tests on concentrically loaded bolted connections susceptible to tearout have been performed in past research. These data have been collected and organized into a database for the purpose of evaluating alternative tearout lengths.

Experimental Database

The experimental database developed for this work includes 899 specimens collected from 20 published works, including this paper. Two types of connections are included: lap splices, in which the bolts are in single shear, and butt splices, in which the bolts are in double shear. A summary of the sources for the experimental data is presented in Table 1.

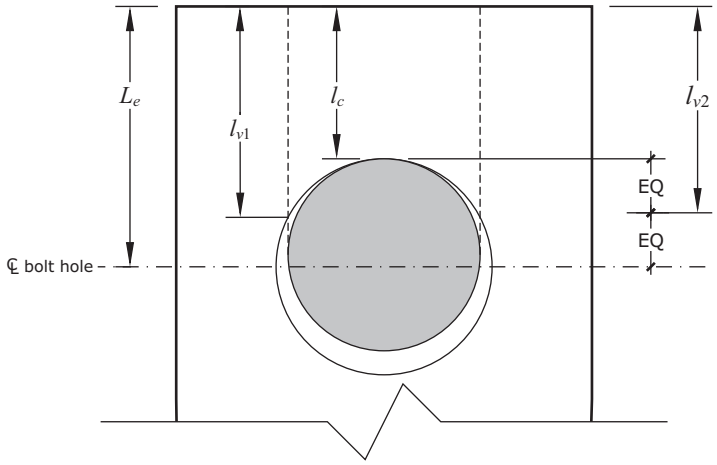

Fig. 2. Tearout length comparison.

Table 1. Summary of Experimental Data Sources			
Reference	**Connection Type**	**Number of Specimens Included in Database**	**Number of Specimens with Bearing, Tearout, or Splitting Failures**
Gillett (1978)	Lap splice	54	33
Frank and Yura (1981)	Butt splice	16	6
Sarkar (1992)	Lap splice	19	2
Karsu (1995)	Lap splice	64	38
Kim and Yura (1999)	Lap splice	41	41
Lewis and Zwerneman (1996)	Butt splice	92	87
Udagawa and Yamada (1998)	Butt splice	219	47
Puthli and Fleischer (2001)	Butt splice	25	9
Rex and Easterling (2003)	Butt splice	31	20
Udagawa and Yamada (2004)	Butt splice	42	5
Freitas (2005)	Butt splice	29	26
Brown et al. (2007)	Butt splice	94	63
Cai and Driver (2008)	Butt splice	44	23
Može and Beg (2010)	Butt splice	38	16
Može and Beg (2011)	Butt splice	24	14
Draganić et al. (2014)	Lap splice	9	0
Može and Beg (2014)	Butt splice	19	8
Teh and Uz (2016)	Lap splice	10	10
Wang et al. (2017)	Butt splice	24	18
This paper	Butt splice	5	5
Total		**899**	**471**

To be included in the database, either the ultimate load, $R_{exp,u}$, or load at ¼-in. deformation, $R_{exp,d}$, must have been recorded. For specimens where $R_{exp,d}$ was not specifically reported, but a plot of the load-deformation response of the connection was provided, the load at ¼-in. deformation was interpolated from the plot. If the specimen reached its peak load prior to attaining ¼-in. deformation, $R_{exp,d}$ was set equal to the ultimate load. Accordingly, $R_{exp,d}$ should be interpreted as a failure load at which peak strength is attained or the connection experiences ¼-in. deformation, whichever occurs first.

Additionally, material testing must have been conducted to determine the tensile strength, F_u, of the connected material in which failure occurred. Only specimens with standard holes were included in the database. A few specimens with slotted holes were identified and were evaluated separately. Connections with composite materials, with cold-formed steel, or subjected to high-temperature testing were not included.

Fields in the database consist of geometric properties (e.g., bolt diameter, plate thicknesses, and edge distances), material properties (e.g., tensile strength and bolt grade), and failure information (e.g., failure mode, $R_{exp,d}$, $R_{exp,u}$, and deformation at $R_{exp,u}$), as well as other relevant information such as bolt installation method.

Only connections categorized as failing in bearing, tearout, or splitting were utilized in this work. The limit state of splitting is distinct from the limit state of tearout. Equations have been proposed to predict splitting strength (Duerr, 2006) and some standards treat tearout and splitting separately (e.g., ASME, 2017). However, splitting is not recognized within the AISC *Specification* (AISC, 2016). Therefore, equations for the limit state of tearout are implicitly covering splitting as well. This approach is justified because experimental results have shown the two limit states to have similar strengths and splitting failures are typically included in the evaluation of the tearout equations, as is done in this work.

Of the 899 specimens in the database, 471 failed in bearing, tearout, or splitting as documented in Table 1. The remaining specimens experienced other failure modes including bolt shear rupture, tensile yielding, tensile rupture, and curling.

Table 2. Test-to-Predicted Ratio Statistics for Various Evaluations of the Load at ¼-in. Deformation for Single-Bolt Specimens (data from 223 specimens, data from 192 specimens meeting minimum edge distance requirements in parentheses)					
	C_t	l_x	C_b	Mean TTP	COV TTP
Current equations	1.2	l_c	2.4	1.223 (1.180)	0.186 (0.172)
Current coefficients	1.2	l_{v1}	2.4	0.952 (0.953)	0.137 (0.144)
Current coefficients	1.2	l_{v2}	2.4	0.992 (0.988)	0.140 (0.147)
Optimized coefficients	1.63	l_c	2.29	0.957 (0.934)	0.153 (0.144)
Optimized coefficients	1.17	l_{v1}	2.36	0.975 (0.976)	0.137 (0.144)
Optimized coefficients	1.23	l_{v2}	2.36	0.975 (0.972)	0.137 (0.144)

Strength of Single-Bolt Specimens

Specimens with a single bolt in the direction of force allow for a direct evaluation of individual limit states. These specimens are evaluated separately from specimens with multiple bolts in the direction of force which may experience multiple limit states (e.g., bearing and tearout). Of the 471 specimens in the database with bearing, tearout, or splitting failures, 313 contained a single bolt in the direction of force. Of these single-bolt specimens, $R_{exp,d}$ was available for 223, $R_{exp,u}$ was available for 301, and both loads were available for 211 of the specimens. The analysis included 265 specimens with one bolt perpendicular to the line of force and 48 with two bolts perpendicular to the line of force. These specimens include many that do not meet the minimum edge distances of AISC *Specification* Table J3.4 (AISC, 2016). Additionally, not all specimens met the AISC *Specification* requirement for bolt installation (i.e., installed to a snug-tight condition or pretensioned).

Experimentally obtained strengths are compared to strengths computed from various instances of a generic bearing and tearout strength equation given by Equation 8.

$$R_n = C_t l_x t F_u \le C_b dt F_u \quad (8)$$

where C_t is the coefficient applied to the tearout strength, C_b is the coefficient applied to the bearing strength, and l_x is the length used for determining tearout strength (i.e., either l_c, l_{v1}, or l_{v2}).

The test-to-predicted ratio (TTP) for each specimen is computed as the ratio of the experimentally obtained strength to the strength from Equation 8 for various selections of C_t, l_x, and C_b. The mean and coefficient of variation (COV) of the test-to-predicted ratio across the specimens is presented in Table 2 for comparisons to the load at ¼-in. deformation and Table 3 for comparisons to the ultimate load. Two values of the mean and COV are presented. The value outside the parentheses includes data from specimens that did not meet the minimum edge distances of AISC *Specification* Table J3.4 (AISC, 2016). The value inside the parentheses excludes specimens that did not meet the minimum edge distances. Note that Table J3.4 has a footnote that permits lesser edge distances, this footnote was not considered in this work.

The data is also presented in Figure 3, where the experimentally obtained strength is normalized against the value of dtF_u and plotted against normalized edge distance. Where the specimen included multiple bolts perpendicular to the direction of load, the experimental strengths were divided by the number of bolts in the connection, n, for plotting purposes.

Optimized coefficients are among the instances of Equation 8 that are compared in Table 2, Table 3, and Figure 3. Six sets of optimized coefficients were computed, one for each of the three tearout lengths (i.e., l_c, l_{v1}, and l_{v2}) at the ultimate and ¼-in. deformation levels. The coefficients were obtained using a numerical optimization to minimize the sum of the square of the difference between the test-to-predicted ratio and unity over all specimens. Single-bolt and multiple-bolt specimens were included in the optimization.

The mean test-to-predicted ratio for the current equations is 1.223 for single-bolt specimens and 1.180 for single-bolt specimens meeting minimum edge distance requirements (Table 2), indicating that current provisions for bearing and tearout are conservative in predicting the load at ¼-in. deformation. This is also seen in Figure 3(b), where most experimental data are above the line representative of current design equations. This is especially true for specimens with smaller edge distances. Either of the two alternative tearout lengths (i.e., l_{v1} or l_{v2}) provides a more accurate and precise assessment of strength when using the current coefficients as seen in both a mean value of the test-to-predicted ratio that is closer to unity and a COV of the test-to-predicted ratio that is lower than for the current equations. However, the use of l_{v1} with current coefficients somewhat overestimates the strength. Results with the optimized coefficients indicate that current coefficients are generally appropriate for use with l_{v1} or l_{v2}.

Similar trends are seen when comparing to the ultimate load (Table 3). A key difference is that the current

Table 3. Test-to-Predicted Ratio Statistics for Various Evaluations of Ultimate Load for Single-Bolt Specimens (data from 301 specimens, data from 234 specimens meeting minimum edge distance requirements in parentheses)					
	C_t	l_x	C_b	Mean TTP	COV TTP
Current equation	1.5	l_c	3	1.065 (1.003)	0.192 (0.140)
Current coefficients	1.5	l_{v1}	3	0.804 (0.812)	0.139 (0.151)
Current coefficients	1.5	l_{v2}	3	0.841 (0.842)	0.133 (0.144)
Optimized coefficients	1.65	l_c	2.95	0.972 (0.921)	0.189 (0.145)
Optimized coefficients	1.16	l_{v1}	3.21	1.009 (1.010)	0.117 (0.128)
Optimized coefficients	1.22	l_{v2}	3.23	1.010 (1.005)	0.120 (0.129)
Rounded coefficients	1.2	l_{v1}	3	0.981 (0.984)	0.119 (0.130)
Rounded coefficients	1.2	l_{v2}	3	1.030 (1.025)	0.120 (0.129)

coefficients with the alternative tearout lengths result in a significant overestimation of strength. Rather, a coefficient of 1.2, the same as is used in the equations for load at the ¼-in. deformation limit state, can provide an accurate prediction of strength with less variation than the current equation.

These results suggest that the difference between the load at ¼-in. deformation and the ultimate load is far smaller than implied by current provisions. Figure 4 shows the ratio $R_{exp,u}/R_{exp,d}$ for single-bolt specimens plotted against the normalized clear distance. The ratio of ultimate load to load at ¼-in. deformation is 1.25 according to the current AISC *Specification* (AISC, 2016) (i.e., the ratio between Equation 4 and Equation 3 equals 1.25). However, the experimental ratios are lower, especially for cases with smaller edge distances. The average ratio of the 211 specimens plotted is 1.05 and only 6 of the specimens have a ratio greater than 1.25.

Strength of Multiple-Bolt Specimens

Of the 471 specimens in the database with bearing, tearout, or splitting failures, 158 have more than one bolt in the direction of force. Of these multiple-bolt specimens, $R_{exp,d}$ was available for 100, $R_{exp,u}$ was available for 136, and both loads were available for 78 of the specimens.

Tables 4 and 5 provide summary statistics for the test-to-predicted ratios computed using the various instances of Equation 8 for multiple-bolt specimens. The values of the COV are approximately the same as those for the single-bolt cases, indicating a good fit of the data. At the ultimate load, when including all specimens, and with rounded coefficients, the mean test-to-predicted ratio is 0.927 for l_{v1} and 0.954 for l_{v2}. These values are lower than that for the single-bolt case and lower than is generally acceptable. A possible reason for this is deformation compatibility between bolts. Achieving the full bearing strength of $3.0dtF_u$ requires significant deformation. It is possible, for example, that by the time the full bearing strength of the interior bolts is achieved, the end bolts have passed their peak strength and contribute only a lower post-peak strength. Nonetheless, when specimens not meeting minimum edge distance and spacing requirements are excluded, the mean test-to-predicted ratios are slightly above unity.

Previous editions of the AISC *Specification* included exceptions to tearout provisions when enough bolts were in a line and certain geometric conditions were met. It was theorized that if the interior bolts fail in bearing, the tearout strength of the end bolt would be less critical. To investigate the effect of neglecting tearout, a test-to-predicted ratio equal to the load at ¼-in. deformation divided by the bearing strength (i.e., the result of Equation 1 times the number of bolts in the connection) is plotted against the normalized clear distance in Figure 5. Only specimens meeting the minimum edge distance and minimum spacing requirements of the current AISC *Specification* (AISC, 2016) are plotted. Specimens that meet the criteria for the tearout exception in the 1993 edition of the AISC *Specification* (AISC, 1993) (i.e., two or more bolts in a line, edge distance greater than $1.5d$, and spacing greater than $3d$) are differentiated with circular markers. The figure shows significant variation; however, many of the specimens have low test-to-predicted ratios, including several that meet the criteria in the 1993 AISC *Specification*.

To summarize, increased accuracy in predicting tearout strength was achieved using either l_{v1} or l_{v2} with a coefficient on the tearout strength of 1.2. This was shown to be true for both the ultimate load and the load at ¼-in. deformation. Based on these initial results, the remaining analyses are conducted with the following equations for tearout strength:

$$R_n = 1.2l_{v1}tF_u \quad (9)$$

$$R_n = 1.2l_{v2}tF_u \quad (10)$$

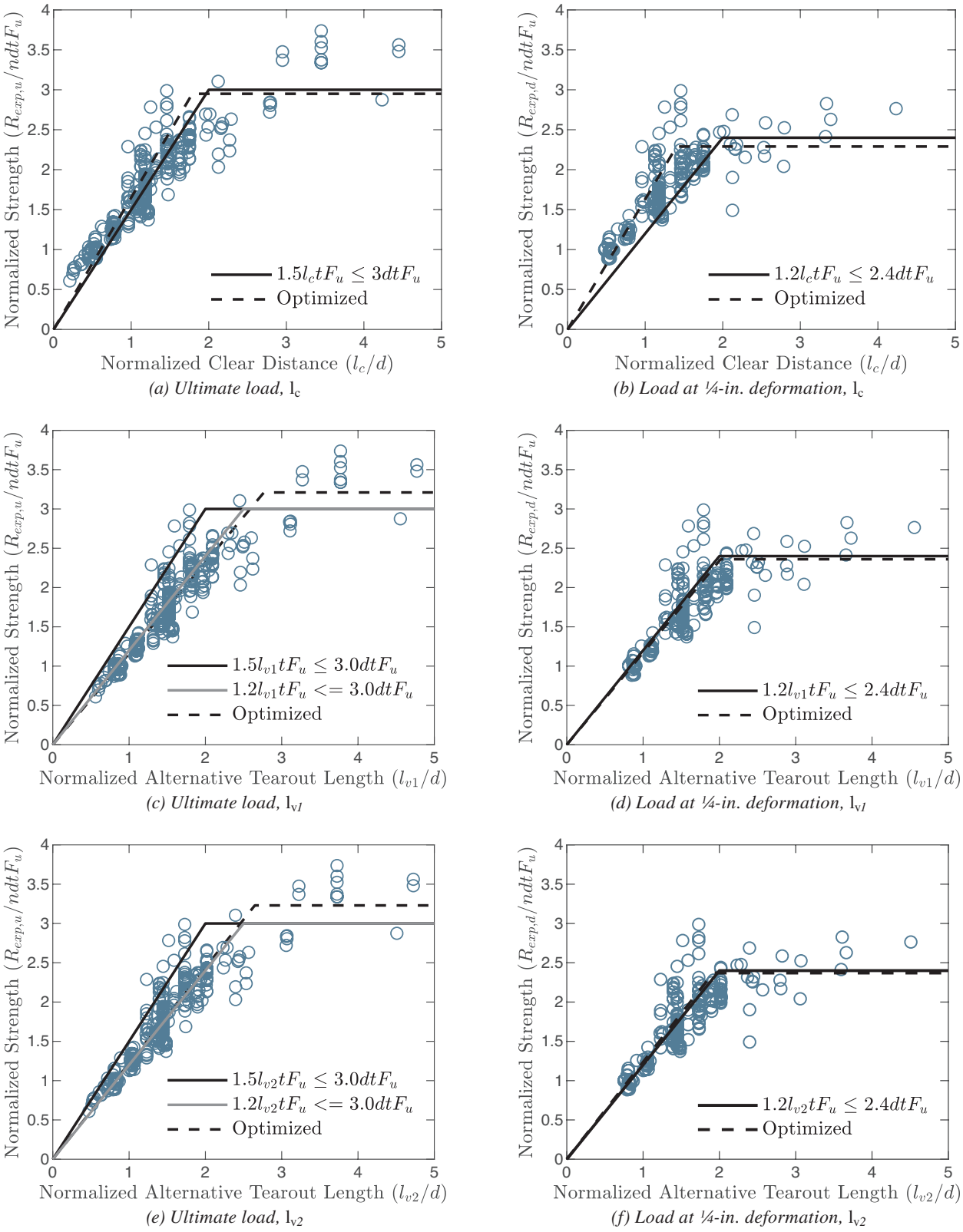

(a) Ultimate load, l_c *(b) Load at ¼-in. deformation,* l_c

(c) Ultimate load, l_{v1} *(d) Load at ¼-in. deformation,* l_{v1}

(e) Ultimate load, l_{v2} *(f) Load at ¼-in. deformation,* l_{v2}

Fig. 3. Normalized strength comparisons between tearout lengths.

Table 4. Test-to-Predicted Ratio Statistics for Various Evaluations of the Load at ¼-in. Deformation for Multiple-Bolt Specimens (data from 100 specimens, data from 62 specimens meeting minimum edge distance and spacing requirements in parentheses)					
	C_t	l_x	C_b	Mean TTP	COV TTP
Current equations	1.2	l_c	2.4	1.137 (1.106)	0.155 (0.159)
Current coefficients	1.2	l_{v1}	2.4	0.973 (1.013)	0.127 (0.126)
Current coefficients	1.2	l_{v2}	2.4	0.992 (1.024)	0.122 (0.127)
Optimized coefficients	1.63	l_c	2.29	1.032 (1.048)	0.122 (0.129)
Optimized coefficients	1.17	l_{v1}	2.36	0.992 (1.033)	0.126 (0.126)
Optimized coefficients	1.23	l_{v2}	2.37	0.995 (1.032)	0.125 (0.127)

Table 5. Test-to-Predicted Ratio Statistics for Various Evaluations of Ultimate Load for Multiple-Bolt Specimens (data from 136 specimens, data from 48 specimens meeting minimum edge distance and spacing requirements in parentheses)					
	C_t	l_x	C_b	Mean TTP	COV TTP
Current equations	1.5	l_c	3	1.011 (1.047)	0.140 (0.172)
Current coefficients	1.5	l_{v1}	3	0.812 (0.951)	0.188 (0.178)
Current coefficients	1.5	l_{v2}	3	0.829 (0.961)	0.182 (0.178)
Optimized coefficients	1.65	l_c	2.95	0.958 (1.029)	0.148 (0.179)
Optimized coefficients	1.16	l_{v1}	3.21	0.937 (1.003)	0.138 (0.164)
Optimized coefficients	1.22	l_{v2}	3.23	0.928 (1.000)	0.140 (0.166)
Rounded coefficients	1.2	l_{v1}	3	0.927 (1.015)	0.145 (0.168)
Rounded coefficients	1.2	l_{v2}	3	0.954 (1.038)	0.144 (0.168)

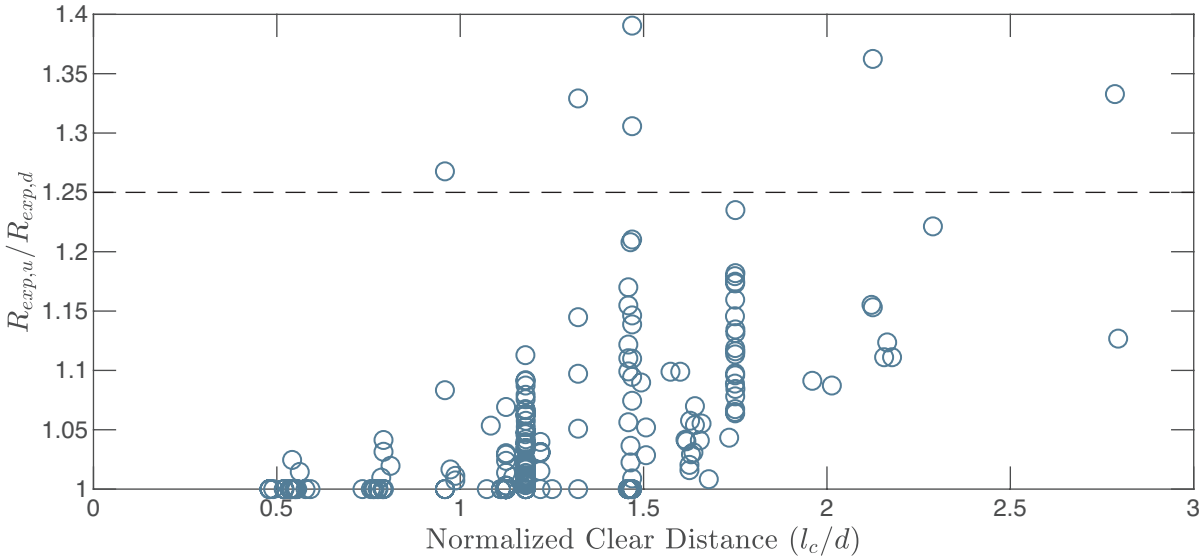

Fig. 4. Ratio of ultimate load to load at ¼-in. deformation versus normalized clear distance.

Table 6. Mean Values of Test-to-Predicted Ratios Based on Level of Tightening			
Load Level	**Pretensioned**	**Snug-Tightened**	**Loose Connection**
Ultimate	1.049	1.023	1.067
¼-in. deformation	1.246	1.197	1.157

Effects of Bolt Tightening

The AISC *Specification* (AISC, 2016) requires that bolts be installed to a snug-tight condition or pretensioned. Many of the experiments in the database utilize untightened bolts or had a gap between the plates. These loose connections do not satisfy the requirements of the AISC *Specification*, but help minimize the contribution of friction to the strength of the connection and better evaluate the strength of the connected material alone.

Frank and Yura (1981) tested connections with different levels of tightening, although loose connections were not considered. They found that specimens with pretensioned bolts had 10% higher strength at ¼-in. deformation when compared to snug-tightened bolts but that the ultimate strength was unaffected by the level of tightening.

Table 6 presents a comparison of experimental strength to strength equations from the current AISC *Specification* (AISC, 2016) for all 471 specimens in the database that failed in bearing, tearout, or splitting. No clearly identifiable trend is seen in the mean test-to-predicted ratios at ultimate load. However, as observed by Frank and Yura (1981), the mean test-to-predicted ratios for the load at ¼-in. deformation tend to increase as the level of tightening increases.

Mixed Failures

Several multiple-bolt specimens tested by Cai and Driver (2008) exhibited mixed failures of bearing or tearout of the end bolts and shear rupture of the interior bolts. This mode of failure is a validation of the premise underlying the use of effective strengths of individual bolts when computing the strength of a bolt group. These specimens were not included in the preceding discussion because they exhibited mixed failures. However, they are examined here to validate the use of the alternative tearout lengths for connections where a mixed failure may occur.

The connected material in which the failures occurred was the web of a wide flange with a measured thickness of 0.36 in. and a measured tensile strength of 74.11 ksi. The connections each had six ¾-in.-diameter bolts (two lines of three) in standard holes. The shear strength of the bolts was measured to be 50.13 kips. Most of these specimens reached their ultimate strength prior to reaching ¼-in. deformation, so only ultimate load was considered. Table 7 summarizes the specimens along with test-to-predicted ratios calculated using different computed strengths.

The test-to-predicted ratios presented in Table 7 were calculated with tearout strength given by the current equation

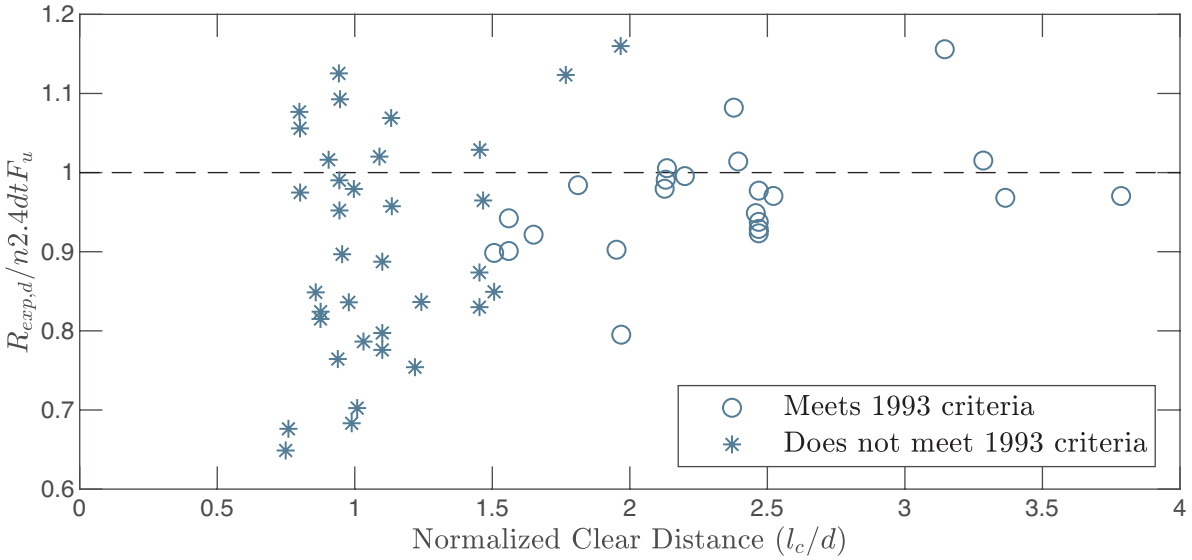

Fig. 5. Test-to-predicted ratio excluding tearout versus normalized clear distance.

Table 7. Analysis of Specimens Tested by Cai and Driver (2008) That Exhibited Mixed Failures						
			Test-to-Predicted Ratio			
Specimen	L_e (kips)	$R_{exp,u}$ (kips)	Using l_c (Eq. 4)[a]	Using l_c (Eq. 4)	Using l_{v1} (Eq. 9)	Using l_{v2} (Eq. 10)
C1E1a	1.00	243.27	0.850	0.981	0.955	0.968
C2E1b	1.00	249.94	0.866	1.005	0.978	0.992
C3E1c	1.00	250.17	0.868	1.007	0.981	0.993
C4E2a	1.25	279.80	0.930	1.044	1.035	1.047
C5E2b	1.26	267.61	0.890	0.993	0.984	0.996
C6E2c	1.26	259.05	0.861	0.965	0.955	0.968
C7E3a	1.50	272.40	0.906	0.946	0.950	0.962
C8E3b	1.50	259.74	0.864	0.903	0.908	0.917
C9E3c	1.51	273.21	0.908	0.947	0.952	0.962
C10E4a	1.76	273.14	0.908	0.908	0.908	0.912
C11E4b	1.75	280.81	0.934	0.934	0.934	0.937
C12E4c	1.75	265.90	0.884	0.884	0.884	0.887
C13E5a	2.00	290.70	0.966	0.966	0.966	0.966
C14E5b	2.00	267.03	0.888	0.888	0.888	0.888
C15E5c	2.01	287.71	0.957	0.957	0.957	0.957
C16E6	2.76	297.49	0.989	0.989	0.989	0.989
		Mean:	0.904	0.957	0.952	0.959

a The predicted strengths for these test-to-predicted ratios were computed without considering potential interaction between the limit states of bearing and tearout and the limit state of shear rupture of the bolt.

(i.e., Equation 4) as well as equations with the alternative tearout lengths (i.e., Equations 9 and 10). Also included in Table 7 are test-to-predicted ratios computed with the predicted strength taken as the lower of the strengths for the bolt group for (1) the limit states of bearing and tearout and (2) the limit state of bolt shear rupture.

The results of these specimens show that it is indeed unconservative to treat bearing and tearout separate from bolt shear rupture, given that doing so results in a 10% overprediction of strength on average. Using this method, specimens C1E1a, C2E1b, and C3E1c were controlled by bearing and tearout strength, and the rest were controlled by bolt shear rupture strength. More accurate but still somewhat unconservative results are obtained when considering the potential of mixed failures and summing the effective strengths of each individual bolt to obtain the strength of the bolt group. Little difference is seen between the use of the clear distance and either of the two alternative tearout lengths, all three result in a 4 to 5% overprediction of strength on average. The remaining error may be due to different bolts achieving their peak strength at different levels of deformation, which is not accounted for in the design equations. Further investigation on deformation compatibility in bolted connections which experience mixed failure is warranted, however, the observed error is small and can be accommodated in the margin of safety.

EXPERIMENTAL STUDY

The evaluation of published experiments showed that tearout equations using l_{v1} and l_{v2} had similarly improved results in comparison to the current equations. The database contains results from hundreds of experiments across a broad range of parameters. However, it only contains specimens with standard holes because the vast majority of concentrically loaded steel bolted connection tests failing in bearing, tearout, or splitting were performed with standard holes.

For connections with standard holes, l_{v1} is greater than l_{v2}. The difference between the two varies only slightly based on the diameter of the bolt, differing by a maximum of 7% for connections that satisfy minimum edge distance requirements and bolts as large as 1.5-in. diameter. The variation is greater, although still relatively small, over a range of hole types. To address this gap in data, a series of experimental tests was conducted to evaluate tearout strength for connections with different hole types.

Test Matrix

Tension tests of 22 single-bolt butt splice connections with different hole types and edge distances were completed. The specimens consisted of two outer pull plates and a single interior test plate as shown in Figure 6. Specimens were designed to fail in bearing, tearout, or splitting of the test plate. Specimens included those with standard holes and holes with minimal clearance, where the value of l_{v1} is greater than l_{v2}. Also included were specimens with oversize holes, holes with ⅛ in. more clearance than oversize holes, and short-slotted holes oriented perpendicular to the load, where the value of l_{v2} is greater than l_{v1}.

The test matrix is presented in Table 8. Two main variables are considered: the type of bolt hole and the edge distance. Four edge distances were investigated for each of the five bolt hole types. Nominal values of the edge distances were 1 in., 1.25 in., 1.5 in., and 2 in. The smallest edge distance (1 in.) is equal to the minimum edge distance permitted by the AISC *Specification* (AISC, 2016) for a ¾-in. bolt in a standard hole. Note that the 1-in. edge distance is not permitted for oversize holes but was used in these tests for consistency. For a ¾-in. bolt in a standard hole, the transition between tearout and bearing occurs at an edge distance of 1.91 in. per current equations. The largest edge distance (2.0 in.) was selected to be somewhat greater than this length and thus provide a comparison to a bearing-controlled failure. Two additional tests beyond the main set of 20 were also completed. Specimen NC2b was a duplicate of NC2a to investigate repeatability. Specimen STD1g

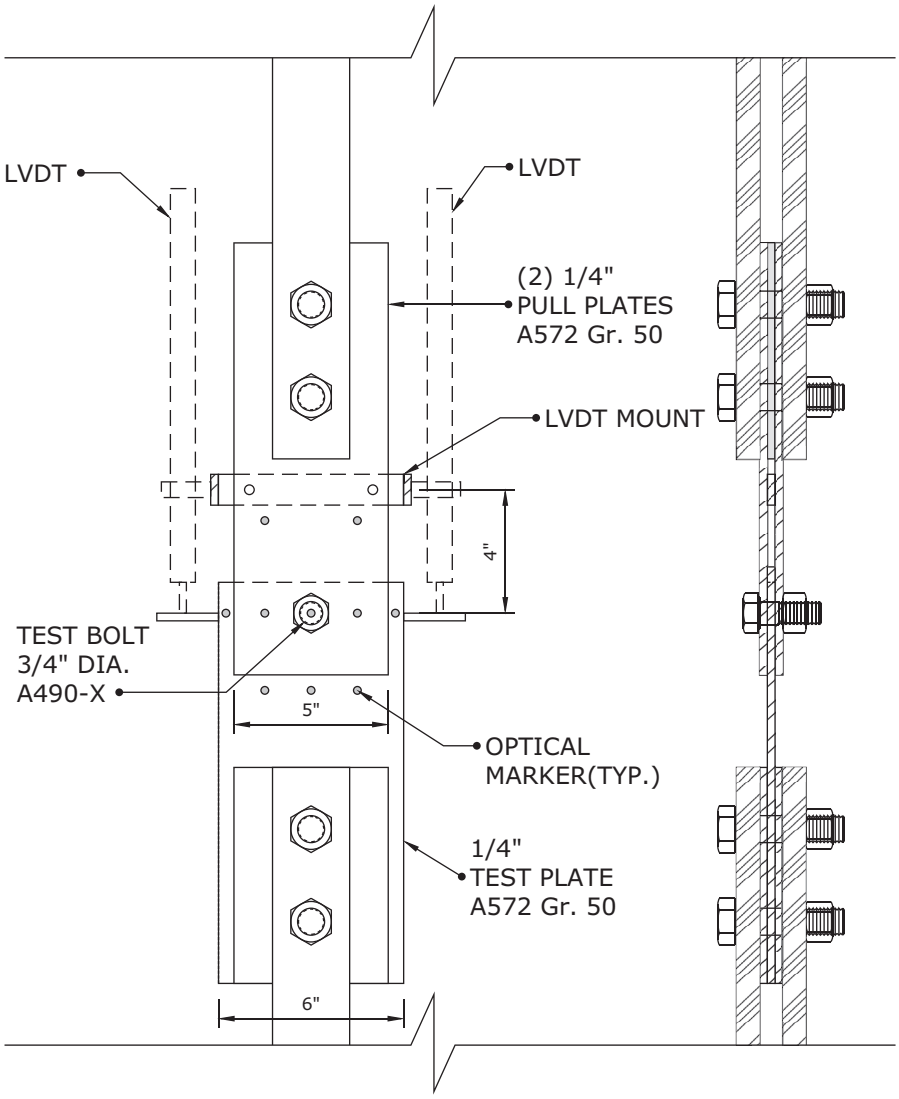

Fig. 6. Experimental test setup.

was a duplicate of STD1, but with the test bolt untightened (instead of in a snug-tight condition) and greased plates to investigate the effect of reduced friction.

Materials and Test Setup

The test plates were ¼-in.-thick ASTM A572 Gr. 50 steel and had a yield strength of 54.5 ksi and a tensile strength of 73.7 ksi, based on the mean of three tensile coupon tests conducted in accordance with ASTM E8 (2016). No special preparation was made to the plate surfaces before testing with the exception of specimen STD1g, where grease was applied to the faying surfaces. The test plates were installed in a universal testing machine and subjected to concentric tension load.

Two linear variable differential transformers (LVDTs) were installed on the test specimen to record movement of the pull plate relative to the test plate over a 4-in. gauge length. The LVDTs recorded the bolt hole deformation as well as elastic deformations of the plates over the gauge length; however, elastic deformations were minimal. An Optotrak optical tracking system was used for supplementary deformation measurements. The optical markers were installed on the test plate, pull plates, and the bolt. Measurements from the optical tracking system were used to verify the LVDT measurements as well as measure elastic elongation of the specimen and pull plate.

After applying a preload of 500 lb to bring the connection into bearing, the test bolt was finger tightened and then brought to a snug-tight condition with a few impacts of an impact wrench. The plies were ensured to be in firm contact. All other bolts were finger tightened. The preload was released prior to applying the main load.

Loading was applied in displacement control at a rate of 0.05 in/min. Most tests were stopped after a near complete loss of load-carrying capacity, typically after one or two loud sounds that likely indicated rupture. To investigate the progression of the failure mechanism, specimens labeled STD1, STD2, STD3, STD4, NC1, NC2b, and SSLT1 were stopped when a steep load drop was seen. Specimen NC2a was stopped even earlier at the first sign of any load drop. All specimens were allowed to achieve their maximum strength.

Results

Load-deformation curves for all specimens are presented in Figure 7. The load at ¼-in. deformation, $R_{exp,d}$, and the ultimate load, $R_{exp,u}$, are presented in Table 8 along with test-to-predicted ratios computed using the current and proposed equations. Measured values were used in calculating the predicted strengths. For specimens with short-slotted holes, l_{v1} was computed graphically with computer-aided drafting software by drawing the specimen using measured dimensions and measuring the length from the edge of the hole to the edge of the material along lines tangent to the bolt. The difficulty in determining l_{v1} in some cases is a drawback for its use in design equations; however, design tables could be developed to alleviate the problem.

Failure Mechanisms

Specimens were disassembled after testing to determine the failure mechanism. Upon disassembly, it was observed that most specimens had a splitting tear as well as shear rupture in the connected material along one or both sides of the bolt hole. For specimens with smaller edge distances (i.e., nominal edge distances of 1 in. and 1.25 in.), the splitting tear extended to the bolt hole, as shown in Figure 8(a). For specimens with larger edge distances, the split did not extend all the way to the bolt hole, as shown in Figure 8(b). Specimens STD4, NC4, STD1g, and NC2b did not exhibit any splitting.

For all specimens that exhibited splitting, it is likely that the initiation of splitting occurred prior to shear rupture in the connected material and coincided with the peak load. Testing of specimen NC2a was stopped shortly after the peak load was attained. Upon disassembly, the initiation of a splitting tear was observed, but no initiation of shear rupture in the connected material was observed. Interestingly, the duplicate specimen, NC2b, did not exhibit splitting failure and achieved a 6% lower strength. The initiation of splitting is seen in the load-deformation curves as a dip that occurs after peak load and flattens out prior to the steeper tearout shear rupture, as depicted in Figure 7.

Strength Evaluation

The means of the test-to-predicted ratios were calculated for each hole type to compare the accuracy of each tearout length, shown in Tables 9 and 10 for the ¼-in. deformation limit state and ultimate limit state, respectively.

The results of Tables 9 and 10 verify the trends identified in the analysis of the previously published experiments. The current tearout equation underestimates the load at ¼-in. deformation, which is much closer to the ultimate load than the equations imply. For load at ¼-in. deformation, differences between the equations using l_{v1} and l_{v2} are shown to be minimal for standard and oversize holes, and both were more accurate than the current equation. Across all hole types, the proposed equation with l_{v1} showed less variation but was unconservative for holes with minimal clearance. The strength of short-slotted holes was underpredicted by the equation using l_{v2}.

Frank and Yura (1981) tested four specimens with long-slotted holes oriented perpendicular to the load. They observed that the initial stiffness and load at ¼-in. deformation was reduced when compared to standard holes but that the ultimate strength, which was controlled by bearing for these specimens, was not reduced. As seen in Figure 7,

Table 8. Test Matrix

		Measured Properties						At ¼-in. Deformation				At Ultimate			
Name	Hole Type	L_e in.	I_c in.	I_{v1} in.	I_{v2} in.	I_{v1}/I_{v2}	d_h in.	$R_{exp,d}$ kips	TTP Using I_c (Eq. 4)	TTP Using I_{v1} (Eq. 9)	TTP Using I_{v2} (Eq. 10)	$R_{exp,u}$ kips	TTP Using I_c (Eq. 4)	TTP Using I_{v1} (Eq. 9)	TTP Using I_{v2} (Eq. 10)
STD1	Standard	1.02	0.615	0.861	0.818	1.052	0.812	19.9*	1.451	1.036	1.091	19.9	1.160	1.036	1.091
STD1g[1]	Standard	0.99	0.578	0.818	0.784	1.044	0.823	17.6	1.359	0.960	1.002	17.8	1.098	0.970	1.012
STD2	Standard	1.16	0.750	0.992	0.954	1.039	0.817	22.9*	1.378	1.042	1.083	22.9	1.103	1.042	1.083
STD3	Standard	1.56	1.157	1.403	1.361	1.031	0.815	31.4*	1.217	1.003	1.034	31.4	0.973	1.003	1.034
STD4	Standard	2.01	1.605	1.846	1.810	1.020	0.818	37.9	1.128	0.912	0.930	43.8	1.042	1.053	1.074
NC1	No clearance	1.03	0.650	0.983	0.838	1.173	0.753	20.7*	1.412	0.933	1.095	20.7	1.129	0.933	1.095
NC2a	No clearance	1.32	0.945	1.278	1.133	1.128	0.752	28.9	1.366	1.010	1.139	29.0	1.097	1.014	1.144
NC2b[2]	No clearance	1.27	0.901	1.240	1.087	1.140	0.744	26.4	1.291	0.939	1.070	27.4	1.070	0.972	1.108
NC3	No clearance	1.56	1.185	1.527	1.373	1.112	0.752	33.2	1.248	0.969	1.078	34.0	1.021	0.990	1.101
NC4	No clearance	2.03	1.661	2.015	1.848	1.091	0.747	41.0	1.218	0.974	0.983	42.4	1.009	1.009	1.019
OVS1	Oversize	1.05	0.584	0.769	0.819	0.940	0.938	20.0	1.537	1.167	1.097	20.3	1.246	1.182	1.111
OVS2	Oversize	1.28	0.813	1.000	1.045	0.957	0.928	24.0	1.298	1.055	1.010	24.4	1.053	1.070	1.024
OVS3	Oversize	1.54	1.079	1.266	1.311	0.965	0.929	29.8	1.223	1.042	1.006	31.0	1.018	1.084	1.047
OVS4	Oversize	2.05	1.590	1.781	1.821	0.978	0.923	36.7	1.088	0.914	0.894	42.0	0.995	1.045	1.022
XOVS1	Extra oversize	0.96	0.427	0.580	0.693	0.838	1.062	14.1*	1.487	1.094	0.917	14.1	1.189	1.094	0.917
XOVS2	Extra oversize	1.29	0.766	0.920	1.030	0.893	1.056	23.3	1.360	1.132	1.012	24.2	1.131	1.177	1.051
XOVS3	Extra oversize	1.51	0.983	1.138	1.247	0.913	1.054	26.2	1.198	1.035	0.945	27.1	0.992	1.071	0.977
XOVS4	Extra oversize	2.04	1.506	1.661	1.771	0.938	1.058	34.7	1.042	0.938	0.880	36.8	0.885	0.996	0.935
SSLT1	Short slot	1.02	0.616	0.730	0.819	0.891	0.812×0.994	18.1*	1.316	1.110	0.990	18.1	1.053	1.110	0.990
SSLT2	Short slot	1.31	0.900	1.015	1.104	0.919	0.816×0.997	21.4	1.096	0.974	0.893	21.8	0.894	0.992	0.911
SSLT3	Short slot	1.56	1.151	1.267	1.353	0.936	0.809×0.990	29.1	1.141	1.038	0.971	29.2	0.917	1.042	0.974
SSLT4	Short slot	2.10	1.700	1.814	1.901	0.954	0.803×0.992	35.0	1.041	0.858	0.833	40.7	0.971	1.000	0.971

* Ultimate load reached prior to 1/4-in. deformation.

1 Duplicate test but bolt was left untightened and plates were greased.

2 Duplicate test to verify repeatability.

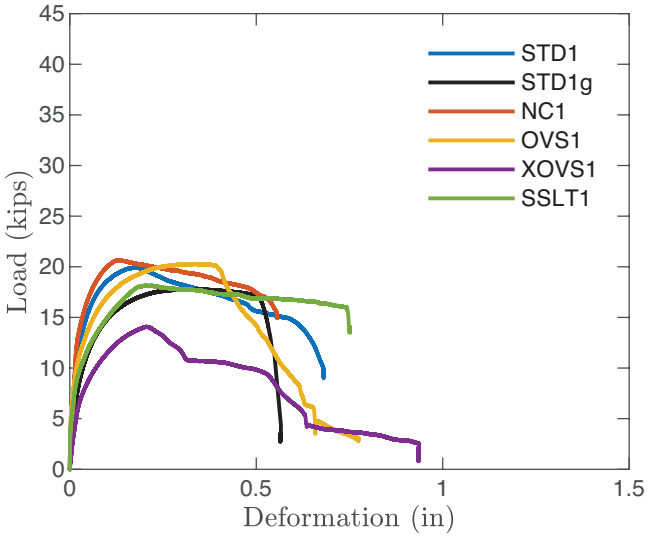

(a) Specimens with nominal edge distance of 1 in.

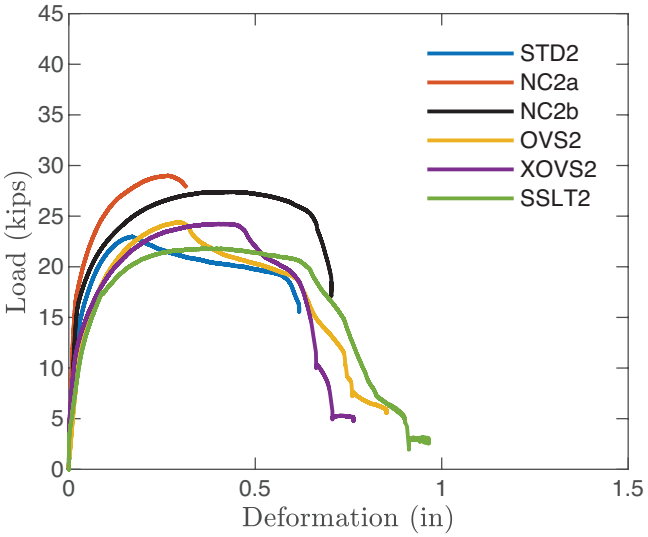

(b) Specimens with nominal edge distance of 1.25 in.

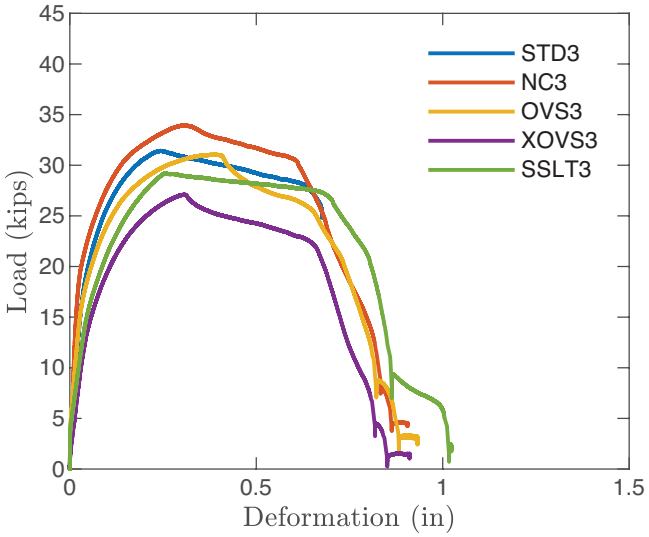

(c) Specimens with nominal edge distance of 1.5 in.

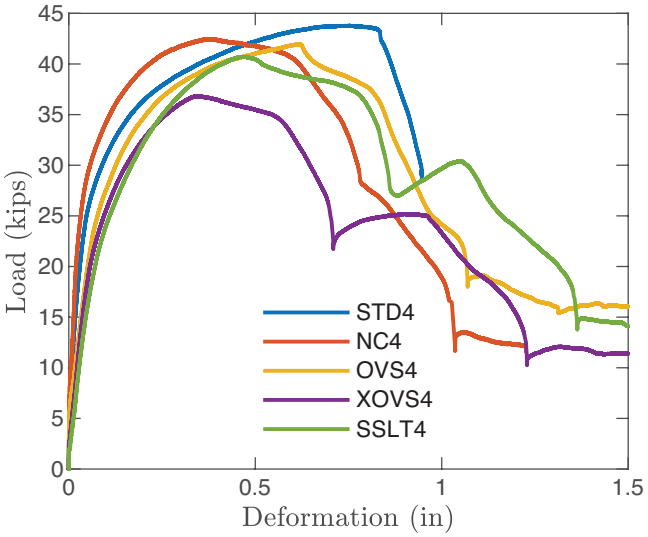

(d) Specimens with nominal edge distance of 2 in.

Fig. 7. Load-deformation curves for experimental tests.

Table 9. Mean Test-to-Predicted Ratio at the ¼-in. Deformation Limit State			
Hole Type	**Using I_c (Eq. 3)**	**Using I_{v1} (Eq. 9)**	**Using I_{v2} (Eq. 10)**
All	1.264	1.008	0.998
STD	1.293	0.998	1.035
NC	1.307	0.965	1.073
OVS	1.286	1.044	1.002
XOVS	1.272	1.050	0.938
SSLT	1.149	0.994	0.922

Table 10. Mean Test-to-Predicted Ratio at the Ultimate Limit State			
Hole Type	**Using I_c (Eq. 3)**	**Using I_{v1} (Eq. 9)**	**Using I_{v2} (Eq. 10)**
All	1.045	1.044	1.032
STD	1.070	1.034	1.071
NC	1.065	0.984	1.093
OVS	1.078	1.095	1.051
XOVS	1.049	1.085	0.970
SSLT	0.958	1.035	0.961

(a) Specimen OVS2 after testing *(b) Specimen OVS3 after testing*

Fig. 8. Photographs of specimens after testing.

the initial stiffness of the specimens with short-slotted holes was among the lowest of those tested in this work. However, both $R_{exp,d}$ and $R_{exp,u}$ were lower for the specimens with short-slotted holes than for the specimens with standard holes.

Although the mean test-to-predicted ratios for the ultimate limit state appear to be accurate for the current equation (Table 10), the results are not consistent across edge distances. This is seen by plotting the test-to-predicted ratios of all tested specimens using the current equation along with the proposed equation using l_{v1} (Figure 9). The linear best-fit lines depict the inconsistency at the ultimate limit state of the current equation across edge distances in comparison to the proposed equation, evident throughout different hole types.

Effect of Bolt Tightening

All but one specimen was tested with the bolt installed to a snug-tight condition. The exception was specimen STD1g, which was nominally identical to STD1 but with the bolt installed loose and grease applied to the faying surfaces so as to investigate the effect of friction. The load-deformation response of specimens STD1g and STD1 is presented in Figure 10.

Several observations can be made from this pair of specimens: (1) The greased specimen was less stiff than the snug-tightened specimens; (2) the load at ¼-in. deformation was 13% greater for the snug-tightened specimen than for the greased specimen; (3) the ultimate load was 12% greater for the snug-tightened specimen than for the greased specimen; and (4) splitting was observed for the snug-tightened specimen, but not the greased specimen.

While these observations were made for a single pair of specimens, the increase in $R_{exp,d}$ corresponds to the increase seen in previous testing data (Table 6). However, the increase in $R_{exp,u}$ was not seen in previous testing data. Also, it is not clear why different failure modes occurred for the two specimens.

RECOMMENDED STRENGTH EQUATIONS

Through the evaluation of existing and new experimental data presented in this work, it was determined that (1) the difference between ultimate load and load at ¼-in. deformation for specimens failing in tearout is less than implied by current equations, (2) current equations for tearout strength underpredict the load at ¼-in. deformation, and (3) current equations are not consistent across edge distances and tend to underpredict the strengths at smaller edge distances. Accordingly, increased accuracy in design can be achieved by replacing AISC *Specification* Equations J3-6c and J3-6d (AISC, 2016) with Equation 9, which utilizes l_{v1}. The equation with l_{v1} was selected since it provides somewhat better results over a wider range of types of bolt holes, particularly short-slotted holes. The same equation but with l_{v2} in lieu of l_{v1} (i.e., Equation 10) would provide similar benefits, and the relative simplicity of calculating l_{v2} may be preferable. A reliability analysis performed in other work confirmed both Equations 9 and 10 to provide a consistent and sufficient level of reliability (Franceschetti, 2020).

An example of the difference between the current and proposed equations is seen in Figure 11. The plotted case is for a single ¾-in.-diameter bolt in a standard hole. The minimum edge distance permitted by the AISC *Specification*

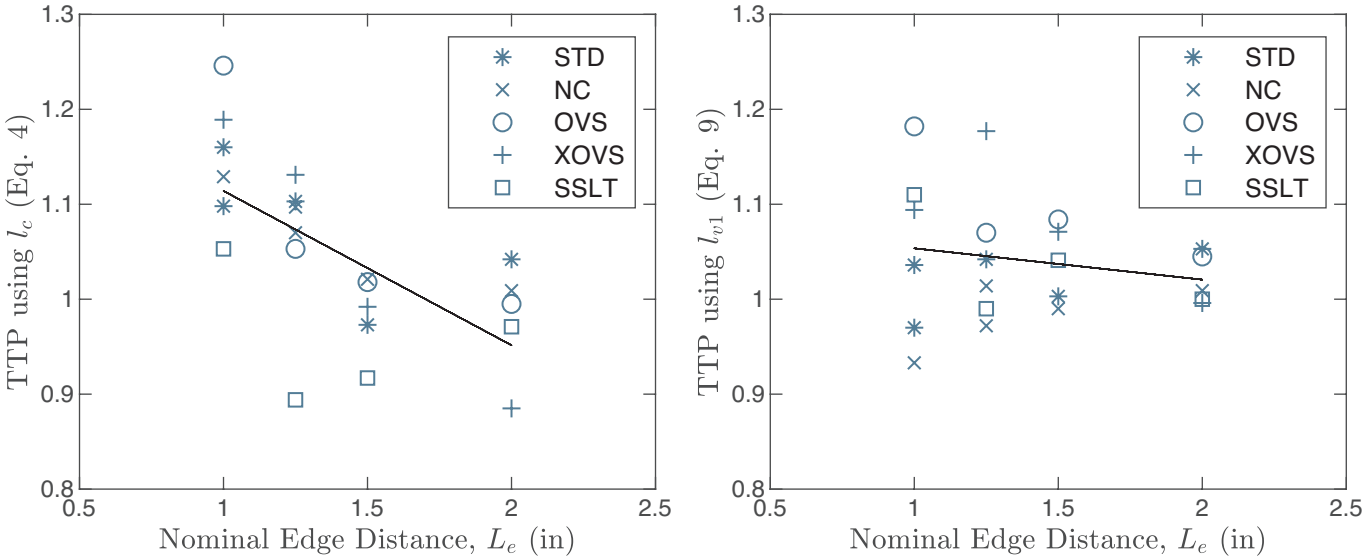

Fig. 9. Test-to-predicted ratios at ultimate limit state with best fit lines.

(1 in.) is shown with a dashed vertical line. Figure 11(a) demonstrates that the equations with the alternative tearout lengths (i.e., Equations 9 and 10) offer additional strength compared to the current equation when deformation at the bolt hole at service load is a design consideration. The difference in strength when deformation at the bolt hole at service load is not a design consideration is less.

While Equation 9 provides increased accuracy over current equations, the computation of the alternative tearout lengths is somewhat more complicated than the computation of the clear distance. This is especially true for eccentrically loaded bolt groups, which are not covered in this work but pose a challenge since the direction of force varies from bolt to bolt. Neither of the alternative tearout lengths have been validated for loads at an angle. The simplicity of the clear distance may continue to be desirable for these situations.

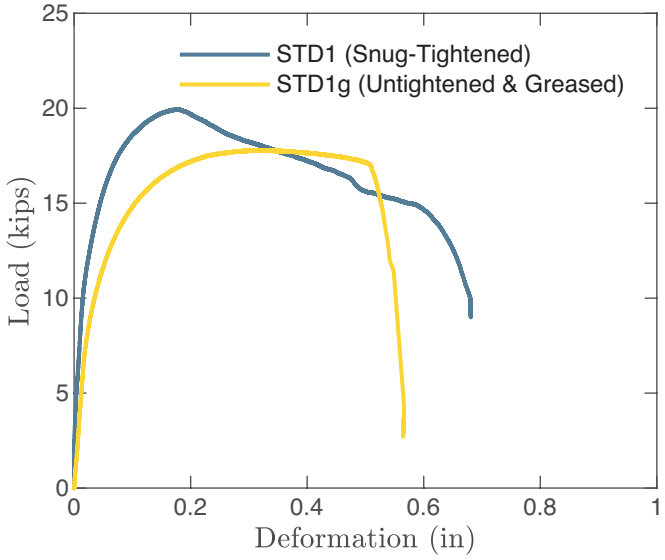

Fig. 10. Snug-tightened specimen versus untightened and greased specimen.

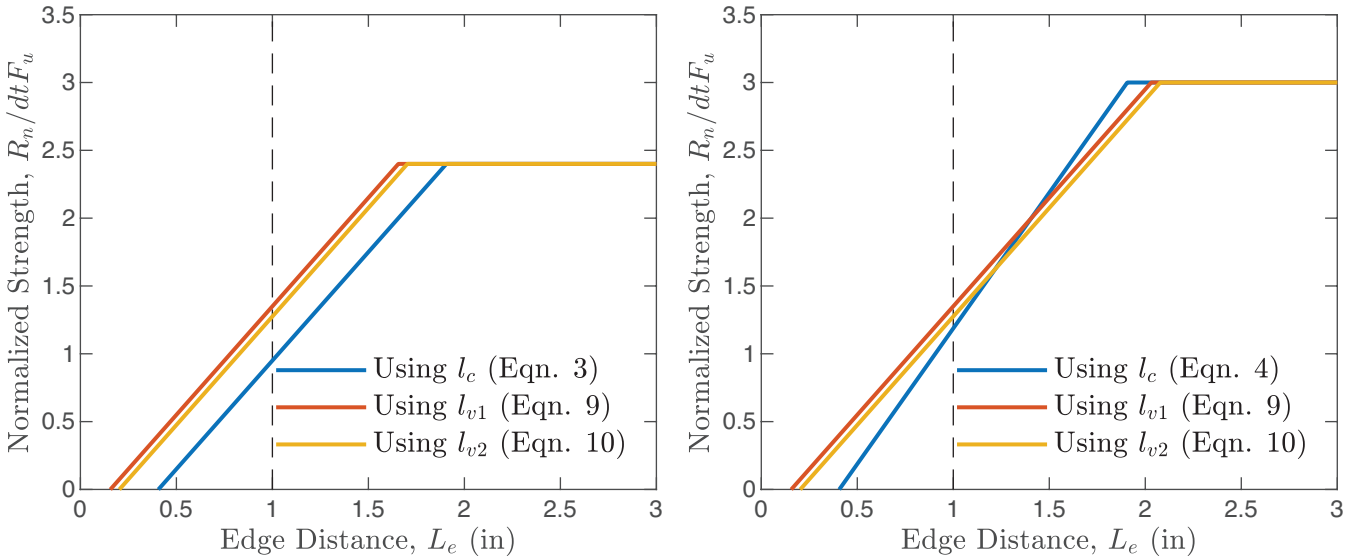

(a) When deformation at the bolt hole at service load is a design consideration

(b) When deformation at the bolt hole at service load is not a design consideration

Fig. 11. Comparison of bearing and tearout strength equations for a ¾-in.-diameter bolt in a standard hole.

CONCLUSIONS

A multifaceted investigation of the limit state of tearout and its impact on design of steel bolted connections has been conducted. Previously published experimental data was evaluated and supplemented with new experimental data to assess the accuracy of current provisions as well as potential alternative provisions. The following conclusions can be made from this work:

- Tearout affects the strength of bolt groups, even for cases of multiple bolts in a row.
- The current equation for tearout strength when deformation at the bolt hole at service load is a design consideration (i.e., load at ¼-in. deformation) is conservative, especially for shorter edge distances.
- The difference between load at ¼-in. deformation and ultimate load for the limit state of tearout is smaller than implied by current provisions.
- Bolt tightening increases the load at ¼-in. deformation. No clear effect of bolt tightening was found on the ultimate load.
- Two alternative tearout lengths, l_{v1} and l_{v2}, were investigated for their potential to improve the accuracy of design equations. Strength equations using these alternative tearout lengths were found to be more accurate than the current equations, which use the clear distance, l_c.
- Design equations with l_{v1} and l_{v2} are similarly accurate for connections with standard and oversize holes. The design equation using l_{v2} was found to be somewhat unconservative for short-slotted holes and holes with clearance greater than oversize. The design equation using l_{v1} was found to be accurate over the entire range of hole types investigated.
- Calculation of l_{v1} is more complicated than l_{v2}, especially for noncircular holes.
- Based on these observations, Equation 9 is recommended for the assessment of tearout strength in concentrically loaded connections. Additional development and validation is necessary for eccentrically loaded connections.

SYMBOLS

C_b Coefficient applied to the bearing strength

C_t Coefficient applied to the tearout strength

F_u Tensile strength of the connected material, ksi

L_e Edge distance measured from center of bolt hole, in.

$R_{exp,d}$ Experimentally determined load at ¼-in. deformation, kips

$R_{exp,u}$ Experimentally determined ultimate load, kips

R_n Nominal strength of connection, kips

d Bolt diameter, in.

d_h Bolt hole diameter, in.

l_c Clear distance from bolt hole edge, in.

l_{v1} Alternative tearout length proposed by Kamtekar (2012), in.

l_{v2} Alternative tearout length proposed by Clements and Teh (2013), in.

l_x General tearout length variable, in.

n Number of bolts

t Thickness of the connected material, in.

ACKNOWLEDGMENTS

Funding for this work was provided by the American Institute of Steel Construction (AISC). The opinions expressed in this work are those of the authors and do not necessarily reflect the views of AISC.

REFERENCES

AISC (1936), *Specification for the Design, Fabrication and Erection of Structural Steel for Buildings*, American Institute of Steel Construction, New York, N.Y.

AISC (1993), *Load and Resistance Factor Design Specification for Structural Steel Buildings*, American Institute of Steel Construction, Chicago, Ill.

AISC (1999), *Load and Resistance Factor Design Specification for Structural Steel Buildings*, American Institute of Steel Construction, Chicago, Ill.

AISC (2010), *Specification for Structural Steel Buildings*, ANSI/AISC 360-10, American Institute of Steel Construction, Chicago, Ill.

AISC (2016), *Specification for Structural Steel Buildings*, ANSI/AISC 360-16, American Institute of Steel Construction, Chicago, Ill.

ASME (2017), *Design of Below-the-Hook Lifting Devices*, American Society of Mechanical Engineers, New York, N.Y.

ASTM E8/E8M-16ae1 (2016), *Standard Test Methods for Tension Testing of Metallic Materials*, ASTM International, West Conshohocken, Pa.

Brown, J.D., Lubitz, D.J., Yavor, C.C., Frank, K.H., and Keating, P.B. (2007), *Evaluation of Influence of Hole Making upon the Performance of Structural Steel Plates and Connections*, Center for Transportation Research, The University of Texas, Austin, Texas.

Cai, Q. and Driver, R.G. (2008), *End Tear-Out Failures of Bolted Tension Members*, Structural Engineering Report No. 278, University of Alberta, Edmonton, Alberta.

Clements, D.D.A. and Teh, L.H. (2013), "Active Shear Planes of Bolted Connections Failing in Block Shear," *Journal of Structural Engineering*, Vol. 139, No. 3, pp. 320–327.

Draganić, H., Dokšanović, T., and Markulak, D. (2014), "Investigation of Bearing Failure in Steel Single Bolt Lap Connections," *Journal of Constructional Steel Research*, Vol. 98, pp. 59–72.

Duerr, D. (2006), "Pinned Connection Strength and Behavior," *Journal of Structural Engineering*, Vol. 132, No. 2, pp. 182–194.

Elliott, M.D., Teh, L.H., and Ahmed, A. (2019), "Behaviour and Strength of Bolted Connections Failing in Shear," *Journal of Constructional Steel Research*, Vol. 153, pp. 320–329.

Franceschetti, N. (2020), "Evaluation of Bolted Connections Susceptible to Tearout," MS Thesis, University of Tennessee, Knoxville, Knoxville, Tenn.

Frank, K.H., and Yura, J. (1981), *An Experimental Study of Bolted Shear Connections*, Report No. FHWA/RD-81/148, Department of Transportation, Washington, D.C.

Freitas, S.T.D. (2005), "Experimental Research Project on Bolted Connections in Bearing for High Strength Steel," Thesis, Delft University of Technology, Delft.

Gillett, P.E. (1978), "Ductility and Strength of Single Plate Connections," PhD Dissertation, The University of Arizona, Tucson, Ariz.

Kamtekar, A.G. (2012), "On the Bearing Strength of Bolts in Clearance Holes," *Journal of Constructional Steel Research*, Vol. 79, pp. 48–55.

Karsu, B. (1995), "The Load Deformation Response of Single Bolt Connections," MS Thesis, Virginia Polytechnic Institute and State University, Blacksburg, Va.

Kim, H.J., and Yura, J.A. (1999), "The Effect of Ultimate-to-Yield Ratio on the Bearing Strength of Bolted Connections," *Journal of Constructional Steel Research*, Vol. 49, No. 3, pp. 255–269.

Lewis, B.E., and Zwerneman, F.J. (1996), *Edge Distance, Spacing, and Bearing in Bolted Connections*, Oklahoma State University, Stillwater, Okla.

Može, P. and Beg, D. (2010), "High Strength Steel Tension Splices with One or Two Bolts," *Journal of Constructional Steel Research*, Vol. 66, No. 8-9, pp. 1,000–1,010.

Može, P. and Beg, D. (2011), "Investigation of High Strength Steel Connections with Several Bolts in Double Shear," *Journal of Constructional Steel Research*, Vol. 67, No. 3, pp. 333–347.

Može, P. and Beg, D. (2014), "A Complete Study of Bearing Stress in Single Bolt Connections," *Journal of Constructional Steel Research*, Vol. 95, pp. 126–140.

Puthli, R. and Fleischer, O. (2001), "Investigations on Bolted Connections for High Strength Steel Members," *Journal of Constructional Steel Research*, Vol. 57, No. 3, pp. 313–326.

Rex, C.O., and Easterling, W.S. (2003), "Behavior and Modeling of a Bolt Bearing on a Single Plate," *Journal of Structural Engineering*, Vol. 129, No. 6, pp. 792–800.

Salmon, C.G., Johnson, J.E., and Malhas, F.A. (2009), *Steel Structures: Design and Behavior*, 5th Edition, Pearson Prentice Hall, Upper Saddle River, N.J.

Sarkar, D. (1992), "Design of Single Plate Framing Connections," Thesis, University of Oklahoma, Norman, Okla.

Teh, L.H., and Uz, M.E. (2016), "Combined Bearing and Shear-Out Capacity of Structural Steel Bolted Connections," *Journal of Structural Engineering*, Vol. 142, No. 11.

Udagawa K. and Yamada T. (1998), "Failure Modes and Ultimate Tensile Strength of Steel Plates Jointed with High-Strength Bolts," *Journal of Structural and Construction Engineering (Transactions of AIJ)*, Vol. 63, No. 505, pp. 115–122.

Udagawa, K. and Yamada, T. (2004), "Ultimate Strength and Failure Modes of Tension Channels Jointed with High-Strength Bolts," *Proceedings of the 13th World Conference on Earthquake Engineering,* Vancouver, British Columbia.

Wang, Y.-B., Lyu, Y.-F., Li, G.-Q., and Liew, J.Y.R. (2017), "Behavior of Single Bolt Bearing on High Strength Steel Plate," *Journal of Constructional Steel Research*, Vol. 137, pp. 19–30.